Journal of Applied Polymer Science

Enhancement in Pyroelectric Properties of PZT-PVA Polymer Nanocomposites with Addition of PAA

Sreekumar Uma, Jacob Philip
Sophisticated Test and Instrumentation Centre, Cochin University of Science and Technology, Cochin 682 022, India
Correspondence to: J. Philip (E-mail: jp@cusat.ac.in)

ABSTRACT: Composites comprising of pyroelectric ceramics and electro-active polymers have gained importance currently as materials for thermal sensing applications, as their unique features and relevant properties can be tailored easily. In this work nanoparticles of PZT have been embedded into PVA/PAA copolymer matrix to form 0 to 3 nanocomposites. Films of the composites are prepared following solvent cast method after dispersing ceramic nanopowder homogeneously in the copolymer matrix with different wt % of the PZT powder. Relevant properties such as dielectric constant and loss factor, pyroelectric coefficients, thermal conductivity, and specific heat capacity as well as Shore hardness have been measured. The material figures of merit for pyroelectric detection have also been determined and reported. It is found that pyroelectric sensing properties of a film of the composite with 20 wt % PZT are comparable to those of commercially used β-PVDF film for the same application, but with a lower figure of merit. However, it provides greater mouldability and simpler processibility for the fabrication of bulk sensors and actuators. So this composite can be considered as a potential material for the design and fabrication of mouldable pyroelectric detectors and actuators. © 2014 Wiley Periodicals, Inc. J. Appl. Polym. Sci. **2014**, *131*, 41142.

KEYWORDS: composites; dielectric properties; nanoparticles; nanowires and nanocrystals; sensors and actuators; thermal properties

Received 22 February 2014; accepted 8 June 2014
DOI: 10.1002/app.41142

INTRODUCTION

Pyroelectric materials are of significant interest as they are widely used for the detection of infrared (IR) radiations, with wavelengths ranging between 3 and 5 μm as well as 8 and 14 μm without the need of cooling.[1] Detection of such radiations finds applications in many areas such as thermal imaging, fire detection, motion sensing, and robotics. When a pyroelectric material is heated, the internal electric charges get dispersed and get aligned in such a way that positive and negative poles are formed across the material.[2] This alignment is permanent unless the field is reversed or a mechanical disturbance that generates heat destroys the alignment.

Currently, single crystals like Lithium tantalate ($LiTaO_3$) and Triglycine sulfate (TGS), certain ceramics like Lead zirconate titanate (PZT) and electro-active polymers like β-Polyvinylidene fluoride (PVDF) are the most widely used materials for these applications, on account of their characteristic ferroelectric, piezoelectric, and pyroelectric properties. These materials often require high temperatures for their synthesis and must be cut, lapped and polished down to the required thickness, which involve expensive and cumbersome processes.[3] Moreover, these materials, other than PVDF, are highly brittle, and TGS very sensitive to humidity, which sometimes put restrictions on their usage. Constant demands for more convenient material systems for specific applications have prompted scientists to focus on thin films, especially composite films, rather than bulk ceramics or single crystals.[4] In recent years, a great deal of attention has been paid to develop composite materials for such applications because a combination of two or more materials can lead to performance enhancements.[5] In these materials it is possible to tailor their electrical, thermal and mechanical properties so that the specifications demanded by the application can be met. Recent studies on ceramic-polymer based pyroelectric composites show potential usefulness as IR sensors in terms of large area, light weight, enhanced strength and flexibility.[2] The hybrid properties of such composites comprise of large pyroelectric coefficient of the ceramic material and the excellent mechanical strength, flexibility, formability, and robustness of the polymer. The properties of these composites depend on the following factors; (i) properties of the individual constituents, (ii) volume fraction of each constituent, (iii) polarizability of ceramic particles as well as the polymer matrix, (iv) nature of interconnection between ceramic particles as well as the interaction between particles and the matrix.[6–8] The simplest type of pyroelectric ceramic-polymer composite is one with 0–3 connectivity, which is a composite material comprising of pyroelectric ceramic powder particles embedded in a polymer material as the matrix.

PZT is a well studied ferroelectric ceramic material. Because of its high piezoelectric coefficient and high Curie temperature, PZT has been widely used for transducer applications for years. However, the response voltage of a pyroelectric material is directly proportional to its pyroelectric coefficient and inversely proportional to its permittivity. Although PZT has a large pyroelectric coefficient, its permittivity is also large, giving rise to a relatively low figure of merit for detector performance. Therefore, a combination with a low permittivity material would be one of the ways to enhance the overall pyroelectric sensor performance and efficiency of PZT.

Recent applications of soft materials based on polymer hydrogels, such as PVA (polyvinyl alcohol) and PAA (poly acrylic acid) mixture, provide a new dimension to the science of materials engineering.[9] Electric current sensitive hydro-gels comprising of polymeric materials actuated by electric stimulus seems to be particularly interesting in view of the fact that in such materials mechanical energy is triggered by an electrical signal. This phenomenon may be used for contraction and relaxation of chemo-electro-mechanical actuators, such as artificial muscles.[10] Attempts to develop stimuli responsive gels are complicated by the fact that structural changes, such as those involving changes in shape and volume, are rather slow. An attractive alternative is the development of polymer hydro-gel composites, which show accelerated chemo-electro-active response upon application or removal of an applied external electric field.

Copolymers exhibit advantages over homopolymers in the interfacial region with increase in fracture toughness of a joint (point of contact of polymers).[11] Even though pure PVA is not inherently electro-active, it has been shown that electro-activity can be induced in to it by forming a co-polymer with PAA.[12] In an earlier paper we have shown that electro-activity can be induced in to PVA by dispersing nanoparticles of PZT in to it. However, the concentration of PZT added to pure PVA has been limited to about 3 wt % due to problems of particle agglomeration and high hardness of the composite. At this PZT concentration, the measured pyroelectric coefficient is only about 11 $\mu C\ m^{-2}\ K^{-1}$, which is much lower than 30 $\mu C\ m^{-2}\ K^{-1}$ currently available with commercial PVDF film sensors. Moreover, the pyroelectric figure of merit is too low and the material is hard even at low concentrations of PZT, which limits its application as a practical sensor. We decided to make the PVA matrix inherently electro-active by forming a copolymer with PAA, and further enhance its electro-activity by dispersing nanoparticles of PZT in to it. This article describes fabrication of 0–3 connectivity composite films of PZT nanoparticles dispersed in PVA/PAA mixture following solvent cast method. To tailor the properties of the composites so prepared, the weight percentage of the nanoceramic is varied to enhance their pyroelectric sensing properties. The work aims at evaluating the suitability of electro-active PVA/PAA copolymer as a host for the dispersion of PZT nanopowder and to investigate the performance of the material as IR or thermal sensing elements.

It is found that viscosity of PVA increases considerably with addition of PAA, which enables to increase the filler loading faction to a sizable value.[12] In this work we have been able to increase the PZT loading fraction up to 20 wt % so as to enhance the pyroelectric coefficient of the composite, cast as a film, comparable to β-PVDF film. Another advantage of mixing PVA with PAA is that, while pure PVA in not electro-active, PVA/PAA co-polymer is slightly electro-active. This adds to the overall electro-activity of the composite.

EXPERIMENTAL

A description of various experimental techniques followed in the work, such as sample preparation and various measurements, are given in this section.

Sample Preparation

Preparation of PVA/PAA co-Polymer Matrix. PVA/PAA copolymer solution was prepared by mixing aqueous solutions (1 : 1 ratio) of 10 wt % PVA and PAA solutions.[13] A 10 wt % PVA solution was first prepared by dissolving a definite amount of PVA (Aldrich, molecular weight: 90,000–1, 20,000, degree of hydrolysis: 99 mol %) in deionized water at 90°C. The appropriate weight of acrylic acid monomer (Aldrich) and 1 wt % cross-linker Triallylamine (Aldrich) were directly dissolved and mixed in distilled water with agitation for about 12 h at 60°C. The resulting mixture was then mixed with aqueous PVA polymer solution until it was completely homogeneous. Finally, an appropriate weight percent (10 wt % of PAA monomer) of the initiator Ammonium per sulfate $(NH_4)_2S_2O_8$ (Aldrich) was added to the above highly viscous polymer mixture for free radical polymerization under continuous stirring at 90°C for 2 h resulting in a homogeneous polymer solution.

Preparation of PZT-PVA/PAA Nanocomposites. PZT nanoparticles were prepared by hydrothermal method described elsewhere.[14,15] PZT nanopowder of required weight percentage was dispersed in the prepared PVA/PAA copolymer solution and was stirred at a constant temperature of 60°C. The resulting gelatinous polymer–ceramic solution was then poured in to a specially designed PTFE container of 1 mm uniform depth. A uniform film of thickness 0.4–0.5 mm was obtained by solvent casting when the excess water got evaporated slowly by keeping it in an oven whose temperature was maintained at 75°C.

The samples prepared had the following weight percents of PZT: 0.5, 1, 2, 3, 5, 10, 15, and 20. A sample of pure PVA/PAA copolymer film was also prepared following the same procedure for comparison.

Sample Characterization and Measurements

Nanocomposite samples of PZT-PVA/PAA as well as pure PVA/PAA copolymer were subjected to powder X-ray diffraction (Bruker, Model D8 Advance) with Cu Kα radiation. The surface morphology of PZT nanopowder and the composites were characterized using TEM (Jeol, Model JEM 2100) and SEM (Jeol, Model 6390 LV), respectively. For dielectric measurements, the nanocomposite film samples were cut in the form of circular pieces of diameter 10 mm and the top and bottom surfaces were electroded with silver paste for measurements. The dielectric properties, dielectric constant and dielectric loss, of the film samples were measured employing an Impedance analyzer (HP,

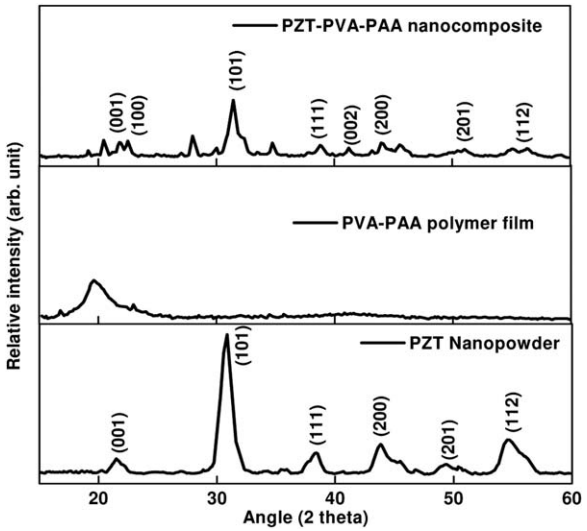

Figure 1. XRD patterns of pure PZT nanopowder, pure PVA/PAA copolymer and 1 wt % PZT-PVA/PAA composite.

Model 4194) in the frequency range 100 Hz to 1 MHz at room temperature.

Another set of specimen was poled following corona discharge method for pyroelectric measurements. First the specimen was pre-heated at a temperature of about 60°C and then subjected to corona discharge by applying a high electric field of 5 kV mm^{-1} for 10 min. The heater was then turned off while maintaining corona discharge till temperature of the specimen reached room value. To measure the pyroelectric coefficients of poled samples, the Byer–Roundy method was employed. Pyroelectric current was measured using a Keithley 485 auto-ranging picoammeter by heating the sample at a steady heating rate of 1°C min^{-1}. The photopyroelectric method (PPE) was used to determine the thermal transport properties, thermal diffusivity (α) and thermal effusivity (e), by measuring the frequency dependence of the PPE signal amplitude and phase in a photopyroelectric spectrometer.[16,17] From the values of α and e, the thermal conductivity (k) and specific heat capacity (c) of the samples were obtained. The Shore D hardness for the samples, including pure PVA/PAA co-polymer, was measured following an indentation technique, measuring the penetration depth of a durometer indenter with a Shore hardness meter (Hardmatic Mitutoyo, Model 321JAA283).

To determine the efficiency of a given material for pyroelectric detector applications, the figures of merit are defined. By using the foregoing electrical parameters, the following material figures of merit are generally defined for assessing the material characteristics of a single element pyroelectric detector, operating in an optimum manner.[18]

$$\text{Current sensitivity}, \quad F_I = p/c \tag{1}$$

$$\text{Voltage responsivity}, \quad F_V = p/c\varepsilon' \tag{2}$$

$$\text{Detection sensitivity}, \quad F_D = p/c\,(\varepsilon'')^{1/2} \tag{3}$$

The pyroelectric figure of merit for each of the samples has been evaluated using the expression

$$\Theta = p(T)/ck\varepsilon' \tag{4}$$

where p, c, k, ε', and ε'' are the pyroelectric coefficient, specific heat capacity, thermal conductivity, dielectric constant, and dielectric loss respectively.

RESULTS AND DISCUSSION

X-ray Powder Diffraction

Figure 1 shows the powder XRD patterns of pure PZT, pure PVA/PAA co-polymer, and 1 wt % PZT-PVA/PAA nanocomposite. The XRD pattern of PZT nanopowder matches well with that of $Pb_{0.52}Zr_{0.48}O_3$ (JCPDS Card No: 33–0784). The average diameter of particles, calculated using the Debye–Scherer formula, is in the range 10–15 nm. The X-ray diffraction measurements performed on pure PVA/PAA copolymer shows that the sample exhibits a peak at angle 2θ of 20°. The intensity of PVA peak decreased when PAA is added, implying that the amorphous region within the PVA/PAA copolymer become dominated. The broad amorphous hump indicates that PVA/PAA copolymers are, in general, amorphous. The amorphous characteristics of the PVA/PAA polymer can greatly enhance the ionic conductivity due to the flexibility of local chain segmental motion in the polymer matrix.[19,20] The XRD patterns of PZT-PVA/PAA composite specimens show presence of peaks corresponding to both PVA/PAA co-polymer and PZT ceramic separately, as expected in a 0–3 ceramic–polymer composite.

Electron Microscope Images

TEM image of PZT nanopowder is shown in Figure 2(a), which consists mainly of homogeneous and spherical grains with an

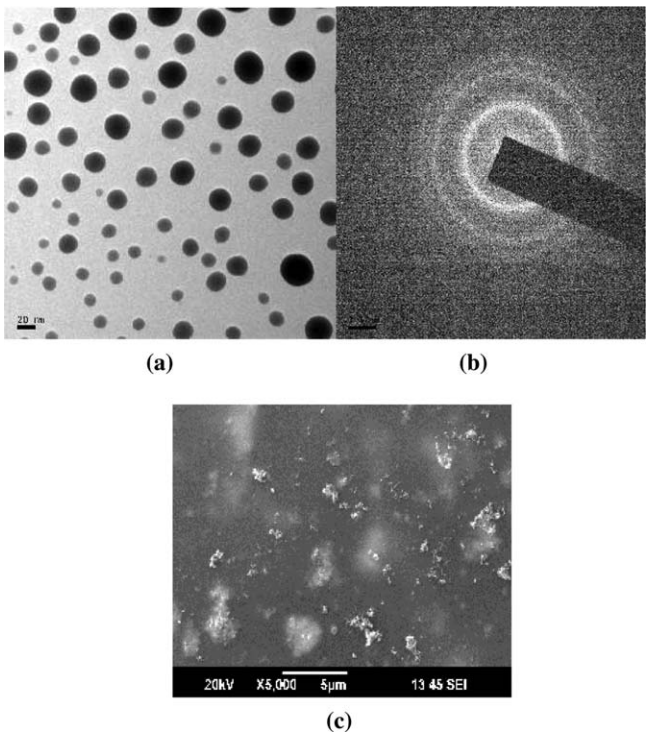

Figure 2. (a) TEM image of PZT nanopowder (b) Selected area diffraction pattern of PZT nanopowder (c) SEM image of 5 wt % PZT-PVA/PAA nanocomposite.

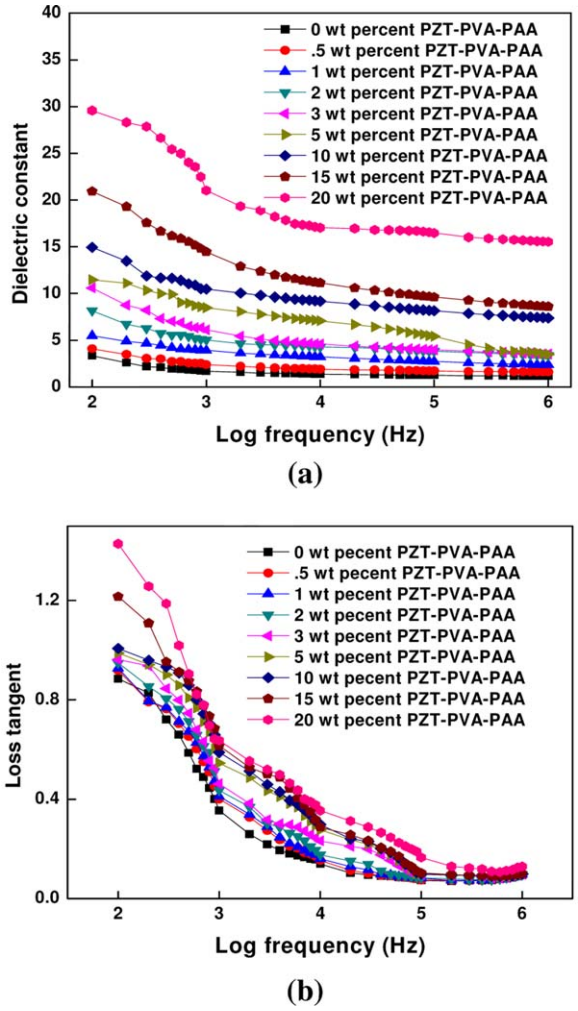

Figure 3. Variation of (a) dielectric constant and (b) loss factor with frequency for PZT-PVA/PAA nanocomposites with different wt % of PZT. [Color figure can be viewed in the online issue, which is available at wileyonlinelibrary.com.]

average diameter in the range 15–25 nm. The selected area diffraction pattern of PZT nanopowder, shown in Figure 2(b), reveals that PZT grains are not monocrystalline but polycrystalline.

The SEM image of 5 wt % PZT-PVA/PAA composite is shown in Figure 2(c). Nanoparticles always show a tendency for aggregation in the nanocomposites due to the large specific surface area and gel viscosity; so there is an increase in the particle size of PZT powder, which is clear from the figure. However, since we make use of the aggregate properties of the material for applications, we do not think that particle agglomeration to the extent seen in the images will affect the bulk properties of the composite.

Dielectric Properties

The variations of dielectric constant and dielectric loss factor with frequency for the composite samples with different concentrations of nano PZT, as well as for pure PVA/PAA, are shown in Figure 3(a,b), respectively. The dielectric permittivity

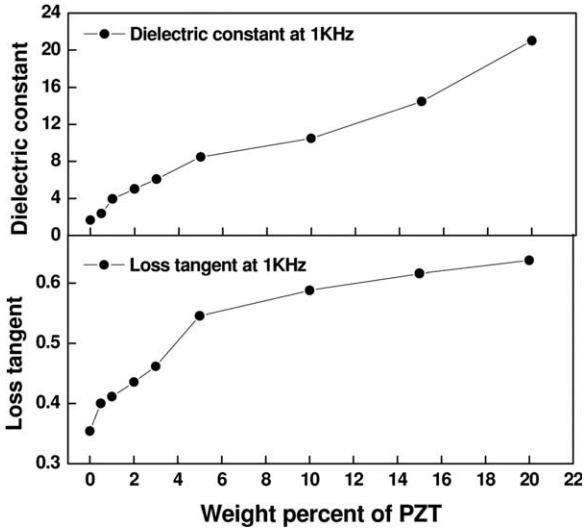

Figure 4. Variations of dielectric constant and loss factor with wt percent of PZT for PZT-PVA/PAA nanocomposites at 1 kHz.

of nanocomposites with varied weight percents of PZT exhibit good stability in the frequency range 1 kHz to 1 MHz.

The variations of dielectric constant and loss tangent with concentration of PZT, at frequency 1 kHz, are shown in Figure 4. It can be noted that the dielectric constant as well as loss factor increase as the PZT content in the PVA/PAA matrix increases. The increase in dielectric constant with increase in PZT content can be attributed to the increase in internal polarization of the sample. However, compared to the large permittivity of pure PZT ceramic, the enhancement of the dielectric permittivity of the nanocomposites is not very significant as the weight percentage of PZT increases. This phenomenon can be attributed to the large difference in the dielectric permittivity between ceramic particles and the copolymer matrix.[21] As PZT has a large dielectric permittivity (>100 at 1 kHz), much higher than the PVA/PAA matrix (<10 at 1 kHz), most of the electric energy is stored in the average field areas in the PVA/PAA matrix with little of the energy being stored in areas around the PZT filler when the filler concentration is low, which is not beneficial to the enhancement of dielectric permittivity.[22,23] The increase in the dielectric loss with increasing PZT content can be attributed to the formation electric dipoles in the medium. In the hydro-gel composite at low frequencies the conduction losses dominate over the domain losses and hence the tan δ loss is high at low frequencies.

Pyroelectric Coefficients

Figure 5 shows the temperature dependence of pyroelectric coefficient (p) of 0–3 composites with various wt % of PZT in the copolymer matrix. The figure depicts that all the poled samples are functional as pyroelectric. Figure 6 shows the variation of pyroelectric coefficient with the loading fraction of PZT in PVA/PAA matrix measured at room temperature. It is found that pyroelectric coefficient increases with the increase of wt % of PZT. A non-zero value of $\approx 2\ \mu C\ m^{-2}\ K^{-1}$ for pyroelectric coefficient for pure PVA/PAA indicates that this material is

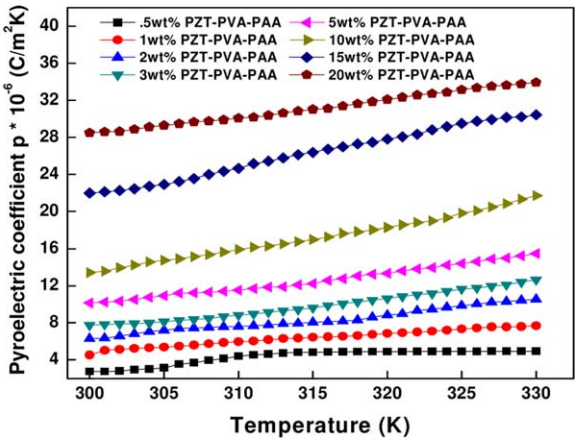

Figure 5. Variations of pyroelectric coefficients with temperature for different samples of PZT-PVA/PAA nanocomposites. [Color figure can be viewed in the online issue, which is available at wileyonlinelibrary.com.]

electro-active. It may be noted that pyroelectric coefficient of 20 wt % PZT-PVA/PAA composite is close to that of β-PVDF.

Thermal Properties by PPE Technique

Though all the thermal transport properties including thermal diffusivity and thermal effusivity have been determined employing PPE technique, since our interest has been only on thermal conductivity and specific heat capacity, results on these alone are reproduced here. Variations of thermal conductivity and specific heat capacity with weight percent of PZT for PZT-PVA/PAA nanocomposites at room temperature are plotted in Figure 7. It can be seen that specific heat decreases with wt % of PZT, while thermal conductivity shows a corresponding increase.

The higher thermal conductivity and lower heat capacity of PZT compared to those of PVA/PAA copolymer explain the variations shown in Figure 7. These variations are in tune with the mean field approximation following rule of mixtures applicable to two-component systems. The rate of increase of thermal conductivity with wt % of PZT deceases with PZT filler loading because of increased interconnection between PZT nanoparticles

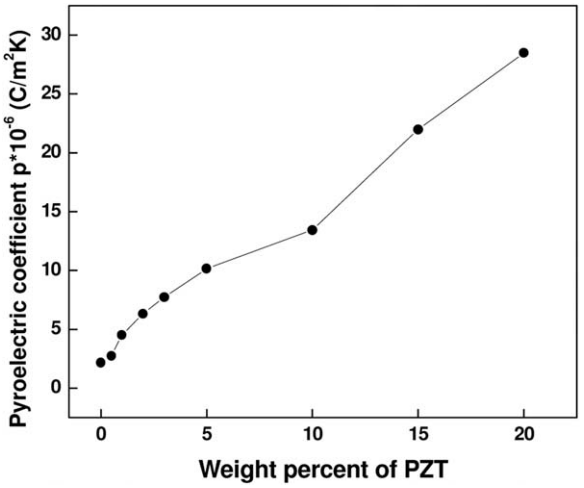

Figure 6. Variation of pyroelectric coefficient with wt % of PZT in PZT-PVA/PAA nanocomposites.

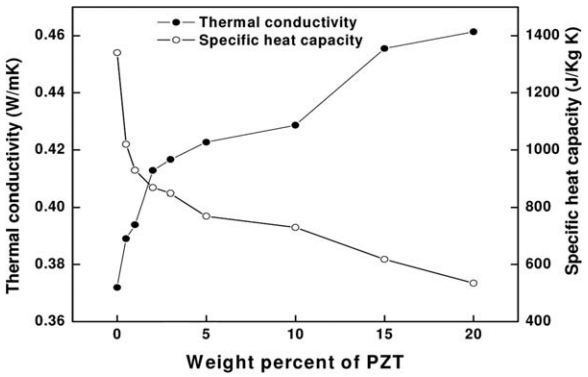

Figure 7. Variations of specific heat capacity and thermal conductivity with weight percent of PZT in PZT-PVA/PAA nanocomposites.

at higher concentrations. A parallel argument explains the observed decrease in specific heat capacity with increase in concentration of PZT.

Shore D Hardness

The variation of Shore D hardness with weight percent of PZT for the composites is plotted in Figure 8. The hardness is found to increase with PZT loading. Because the hardness of a material scales inversely with the flexibility (or formability) of a material, we plotted the inverse Shore D hardness against wt % of PZT. This variation is shown in Figure 9. As is evident from this figure, as the wt % of PZT increases the Shore hardness increases or inverse Shore hardness decreases.

Pyroelectric Figures of Merit

The pyroelectric figures of merit (FOM) determine a material's effectiveness for the detection of IR or thermal radiations. Using eqs. (1)–(4) , values of figures of merit have been determined. The variation of the pyroelectric figure of merit Θ, as defined by eq. (4), with PZT concentration is plotted in Figure 9. It can be noted that the figure of merit (FOM) increases from 25×10^{-10} to 55×10^{-10} as the weight % of PZT increases from 0 to 20. This increase in FOM is due to the corresponding increase in pyroelectric coefficient and decrease in specific heat capacity, though the corresponding increases in dielectric constant and thermal conductivity work against it. The variations of figures of merit (F_I, F_V, and F_D, as defined by eqs. (1)–(3),

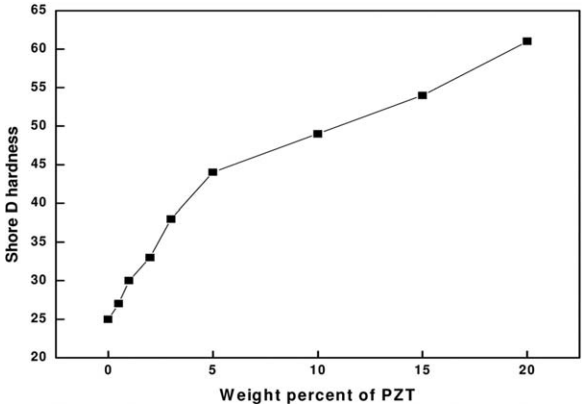

Figure 8. Variations of Shore D hardness with wt % of PZT in PVA/PAA polymer matrix.

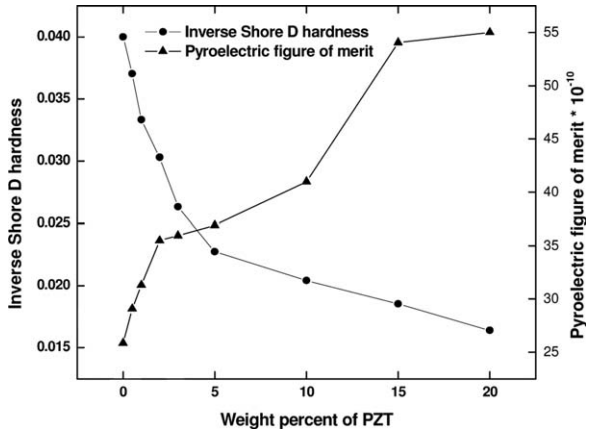

Figure 9. Variations of inverse Shore D hardness and pyroelectric figure of merit [as defined by eq. (4)] with weight percent of PZT in PZT-PVA/PAA nanocomposites.

along with inverse Shore D hardness, against wt % of PZT are plotted in Figure 10. All the figures of merit show considerable increase in their values with increase in PZT content. The variation of inverse Shore D hardness is also plotted in these figures for direct comparison with hardness in each case. The figure of merit F_I (current sensitivity) curve meets inverse Shore D hardness curve at the composition corresponding to 7 wt % PZT. The FOM curves for voltage responsivity, F_V, and detection sensitivity, F_D, intersect the inverse Shore D hardness curve at the composition corresponding to 5 wt % PZT. The inverse Shore D hardness curve meets the pyroelectric FOM [as defined by eq. (4)] curve at the composition corresponding to 4.5 wt % PZT. For this composition a pyroelectric FOM of nearly 36×10^{-10} (or pyroelectric coefficient of nearly 10 μC m^{-2} K^{-1}) corresponds to an inverse Shore D hardness of nearly 0.025 or Shore D hardness of 40) for this composite.

These data provide guidelines for the selection of suitable composite for the envisaged application.

Comparison of PZT-PVA/PAA with PZT-PVA and β-PVDF

The main problem while considering PZT-PVA nanocomposites for pyroelectric detector application is that composites with higher fraction of the ceramic could not be prepared due to the problem of agglomeration. To enhance the loading fraction of the ceramic in the PVA matrix, the polymer matrix has been modified as discussed above. With this modification the loading fraction of PZT could be increased up to 20 wt % while with pure PVA the maximum weight percent that could be prepared was only 3. This can be attributed to the increase in viscosity of PVA/PAA copolymer. Therefore with PZT-PVA/PAA nanocomposites we could obtain films of much higher figures of merit and pyroelectric coefficients.

Another important aspect to be noted is that in the case of PZT-PVA/PAA nanocomposites the rate of increase of pyroelectric coefficient with PZT concentration is smaller compared to the corresponding rate in PZT-PVA composites. However, the advantage lies in that the dielectric constant also shows a similar trend, hence improving the overall pyroelectric figure of merit.

A comparison of the properties of PZT-PVA/PAA and PZT-PVA with those of commercially used β-PVDF sensor seems relevant

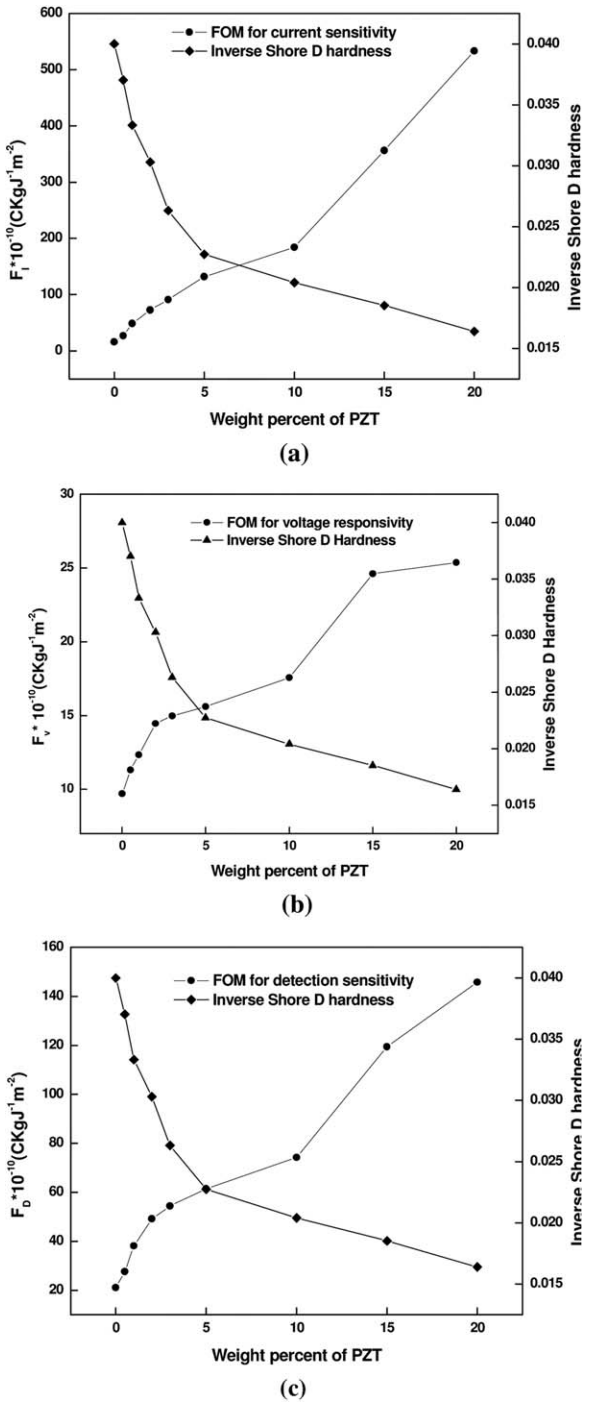

Figure 10. Variations of the figures of merit, (a) current sensitivity (F_I), (b) voltage responsivity (F_V), and (c) detection sensitivity (F_D) [as defined by eqs. (1)–(3)] and inverse Shore D hardness with PZT filler concentration.

at this point. The pyroelectric coefficients, figures of merit and Shore harness values (all at room temperature) for a selected composition of each of these are tabulated in Table I. From this table it is obvious that while the pyroelectric coefficient of 3 wt % PZT-PVA is comparable to 3 wt % PZT-PVA/PAA, the latter has a much higher figure of merit, and the 20 wt % PZT-PVA/PAA provides a much higher pyroelectric coefficient,

Table I. Comparison of Pyroelectric Properties and Hardness of Nanocomposites of PZT-PVA, PZT-PVA/PAA, and Commercial PVDF Film

	Pyroelectric properties and Shore hardness		
Material	Pyroelectric coefficient; p ($\mu C\ m^{-2}\ K^{-1}$)	Pyroelectric figure of merit; $p/ck\varepsilon$ ($x10^{-10}$)	Shore hardness
3 wt %PZT-PVA	10.8	4.5	29.4
3 wt %PZT-PVA/PAA	7.8	35.95	38
20 wt %PZT-PVA/PAA	28.48	55.10	61
B-PVDF film (commercial sensor)	27	112.5	75

comparable to commercially available β-PVDF. Moreover, 20 wt % PZT-PVA/PAA has a comparatively high figure of merit, but less than that of β-PVDF. A lower FOM means lower efficiency of the material as a pyroelectric detector. The hardness also increases with PZT loading, but still 20 wt % PZT-PVA/PAA has hardness lower than commercial β-PVDF. Perhaps by optimizing the preparation conditions it may be possible to further improve the figure of merit of this composite. Possibility to mold the sensor to any shape and its biocompatibility are the advantages we see now for this composite sensor material. Depending on the envisaged application one can make a choice of the material. We do not anticipate any difficulty in casting large area film sensors or bulk three-dimensional sensors or actuators based on PZT-PVA/PAA following the solvent cast method followed in this work.

The data on β-PVDF quoted in Table I are for films of thickness $\approx$28 μm. For sensor applications this material can be used only in the form of films. Preparation of β-PVDF even in the form of films is difficult as chemical preparation or mechanical stretching need to be critically controlled for the formation of the β-phase. To the best of our knowledge, nobody has succeeded in preparing β-PVDF in the bulk form. Though we have reported results on PZT-PVA/PAA nanocomposites prepared in the form of films, there is no difficulty in preparing these in the bulk form suited to applications such as three-dimensional sensors and actuators.

CONCLUSIONS

We have successfully prepared PZT-PVA/PAA nanocomposites with weight percent of nano PZT varying from 0 to 20, and investigated their structural, morphological, dielectric, thermal and pyroelectric properties. Formation of PVA-PAA copolymer enables loading the matrix with much higher concentrations of PZT. The variations of pyroelectric coefficient, Shore hardness as well as pyroelectric figures of merit have been measured with variations in PZT filler loading, and found that pyroelectric properties get significantly enhanced with PZT addition; however it is at the expense of the flexibility of the composite. Because of particle agglomeration and hardness enhancement beyond applicable limits, weight percent of PZT could not be increased beyond 20. For 20 wt % sample, the pyroelectric coefficient obtained is comparable to that of PVDF, which is extensively used currently for commercial applications.

If more flexibility is desired for any application, it automatically puts a limit on the detection sensitivity of the material. Depending on the application, one shall select the material and design the sensor. Based on the results obtained, PZT-PVA/PAA films are proposed as potential candidates for the design and fabrication of thermal and IR sensing elements. In applications requiring bulk detectors with curved surfaces for special applications, one can take advantage of their flexibility and high strength. Moreover, it may be possible to fabricate bulk pyroelectric sensors and actuators of any size and shape with these materials.

ACKNOWLEDGMENTS

Work supported by Department of Science and Technology, New Delhi under Nanomission scheme (SR/NM/NS-30/2010). Sample characterization done at SAIF, STIC, Cochin. One of the authors (SU) thanks Kerala State Council for Science, Technology and Environment for support.

REFERENCES

1. Dorey, R. A.; Whatmore, R.W. *J. Eur. Ceram. Soc.* **2005**, *25*, 2379.
2. Van Vlack, L. H. Elements of Material Science and Engineering, 6th ed.; Prentice Hall: New Jersey, **2002**, p 347.
3. Corker, D. L.; Zhang, Q.; Whatmore, R. W.; Perrin, C. *J. Eur. Ceram. Soc.* **2002**, *22*, 383.
4. Koga, K.; Ohigashi, H. *J. Appl. Phys.* **1986**, *56*, 2142.
5. Ng, K. L.; Helen, L. W. C.; Choy, C. L. *IEEE Trans. Ultrason. Ferroelectrics Freq. Control* **2000**, *47*, 1308.
6. Aggarwal, M. D.; Currie, J. R.; Penn, B. G.; Batra, A. K.; Lal, R. B. NASA/TM-2007–215190.
7. Newnham, R. E.; Skinner, D. P.; Cross, L. E. *Mater. Res. Bull.* **1978**, *13*, 525.
8. Tressler, J. F.; Alkoy, S.; Newnham, R. E. *Compos. A* **1999**, *30*, 477.
9. Nayak, S.; Lyon, L. A. *Angew. Chem.* **2005**, *44*, 7686.
10. Osada, Y.; Gong, J. P. *Adv. Mater.* **1998**, *10*, 827.
11. Carl, A. K. Materials Science in Engineering, 4th ed.; Elsevier Science Series: Amsterdam.
12. Pandey, P. K.; Smitha, P.; Gajbhiye, N. S. *J. Polym. Res.* **2008**, *15*, 397.
13. Wu, G. M.; Lin, S. J.; Yang, C. C. *J. Membr. Sci.* **2006**, *275*, 127.
14. Deng, Y.; Liu, L.; Cheng, Y.; Nan C-W.; Zhao, S. *J. Mater. Lett.* **2003**, *57*, 1675.
15. Uma, S.; Philip, J. *Ind. J. Pure Appl. Phys.* **2013**, *51*, 717.
16. Mandelis, A.; Zver, M. M. *J. Appl. Phys.* **1985**, *57*, 4421.

17. Menon, C. P.; Philip, J. *Meas. Sci. Tech.* **2000**, *11*, 1744.
18. Lal, R. B.; Batra, A. K. *Ferroelectrics* **1993**, *142*, 51.
19. Wright, P. V. *Br. Polym. J.* **1975**, *7*, 319.
20. Fauvarque, J. F.; Salmon, E.; Vassal, N. *Electrochem. Acta.* **2000**, *45*, 1527.
21. Rao, Y.; Qu, J. M.; Marinis, T.; Wong, C. P. *IEEE Trans. Compon. Packag. Technol.* **2000**, *23*, 680.
22. Li, J. Y.; Zhang, L.; Ducharme, S. *Appl. Phys. Lett.* **2007**, *90*, 132901.
23. Ling, A.; Boggs, S. A.; Calame, J. P. *IEEE Trans. Electr. Insul. Mat.* **2008**, *24*, 5.